EDGEWOOD CHEMICAL BIOLOGICAL CENTER
U.S. ARMY RESEARCH, DEVELOPMENT AND ENGINEERING COMMAND
Aberdeen Proving Ground, MD 21010-5424

ECBC-TR-1452

SIGNALING PATHWAYS ASSOCIATED WITH VX EXPOSURE IN MESENCHYMAL STEM CELLS

Daniel Angelini
Christopher Phillips
Amber Prugh
Trevor Glaros

RESEARCH AND TECHNOLOGY DIRECTORATE

Bao Tran

EXCET, INC.
Springfield, VA 22151-2110

September 2017

Disclaimer

The findings in this report are not to be construed as an official Department of the Army position unless so designated by other authorizing documents.

REPORT DOCUMENTATION PAGE

Form Approved
OMB No. 0704-0188

1. REPORT DATE *(DD-MM-YYYY)*	**2. REPORT TYPE**	**3. DATES COVERED** *(From - To)*
XX-09-2017	Final	Mar 2016 – Oct 2016

4. TITLE AND SUBTITLE

Signaling Pathways Associated with VX Exposure in Mesenchymal Stem Cells

5a. CONTRACT NUMBER

5b. GRANT NUMBER

5c. PROGRAM ELEMENT NUMBER

6. AUTHOR(S)

Angelini, Daniel; Phillips, Christopher; Prugh, Amber; Glaros, Trevor (ECBC); and Tran, Bao (Excet)

5d. PROJECT NUMBER

5e. TASK NUMBER

5f. WORK UNIT NUMBER

7. PERFORMING ORGANIZATION NAME(S) AND ADDRESS(ES)
Director, ECBC, ATTN: RDCB-DRB-D, APG, MD 21010-5424
Excet, Inc., 8001 Braddock Road, Suite 303, Springfield, VA 22151-2110

8. PERFORMING ORGANIZATION REPORT NUMBER

ECBC-TR-1452

9. SPONSORING / MONITORING AGENCY NAME(S) AND ADDRESS(ES)
ECBC, FY16 Section 219 Seedling Program, APG, MD 21010-5424

10. SPONSOR/MONITOR'S ACRONYM(S)

11. SPONSOR/MONITOR'S REPORT NUMBER(S)

12. DISTRIBUTION / AVAILABILITY STATEMENT
Approved for public release: distribution unlimited.

13. SUPPLEMENTARY NOTES

14. ABSTRACT (LIMIT 200 WORDS)

Mesenchymal stem cells (MSCs) are multipotent adult stem cells that are key regulators of tissue maintenance and repair. These cells have been identified in several different tissues, but they typically originate in the bone marrow and then circulate through the body in the bloodstream. The U.S. Army Edgewood Chemical Biological Center BioDefense Branch members and academic laboratories have demonstrated that bone marrow-derived MSCs exposed to organophosphate (OP) pesticides sustain significant changes in their ability to proliferate and differentiate. In the literature, OP compounds were shown to affect the activity and expression levels of acetylcholinesterase (AChE); however, it is still unclear whether the effect on AChE is caused by these changes. It is also possible that these OP compounds have other unknown secondary effects on MSCs. In this study, we exposed MSCs to the OP chemical warfare agent 145*O*-ethyl *S*-(2-diisopropylaminoethyl) methylphosphonothioate (VX) and performed phospho-array and phosphoproteomic analysis to gain insights into the signaling pathways associated with VX exposure.

15. SUBJECT TERMS
Mesenchymal stem cell (MSC)
O-ethyl *S*-(2-diisopropylaminoethyl) methylphosphonothioate (VX)
Chemical warfare agent (CWA)
Cell signaling

16. SECURITY CLASSIFICATION OF:			**17. LIMITATION OF ABSTRACT**	**18. NUMBER OF PAGES**	**19a. NAME OF RESPONSIBLE PERSON**
a. REPORT	**b. ABSTRACT**	**c. THIS PAGE**			Renu B. Rastogi
U	U	U	UU	34	**19b. TELEPHONE NUMBER** *(include area code)* (410) 436-7545

Blank

PREFACE

The work described in this report was authorized under the U.S. Army Edgewood Chemical Biological Center (ECBC) FY16 Seedling Program. This work was started in March 2016 and completed in October 2016.

The use of either trade or manufacturer's names in this report does not constitute an official endorsement of any commercial products. The report may not be cited for purposes of advertisement.

This report has been approved for public release.

Acknowledgments

The authors wish to thank Drs. Way Fountain, Nicole Rosenzweig, and Robert Kristovich, (ECBC; Aberdeen Proving Ground, MD); Rebecca Braun (Booz Allen Hamilton; Belcamp, MD); and Davi Kristovich (Excet, Incorporated; Springfield, VA) for scientific and administrative support.

Blank

CONTENTS

FIGURES

TABLES

SIGNALING PATHWAYS ASSOCIATED WITH VX EXPOSURE IN MESENCHYMAL STEM CELLS

1. INTRODUCTION

1.1 Background

Organophosphate (OP) compounds were originally developed as powerful insecticides but were later used as chemical warfare agents (CWAs) (*1, 2*). These highly toxic compounds cause severe toxic effects and are easily absorbed into the body through the skin and mucous membranes. These chemicals act through the inhibition of the enzyme, acetylcholinesterase (AChE), which is responsible for degrading the neurotransmitter molecule, acetylcholine (ACh), within the nervous system (*3*). The inhibition of AChE by OP compounds induces cholinergic hyperstimulation that can lead to respiratory arrest and death (*2–4*) in severe cases. In addition to toxic effects to the nervous system, low-level exposures to OP compounds can cause toxicities in organs and tissues, including lungs (*5, 6*), kidneys (*7*), gastrointestinal tract (*8*), and bone marrow (*9*). The U.S. Army Edgewood Chemical Biological Center (ECBC) BioDefense Branch team members demonstrated that bone marrow-derived human mesenchymal stem cells (MSCs) that are exposed to an OP pesticide (parathion) or its metabolite (paraoxon) are significantly altered in their ability to proliferate and differentiate into adipocytes or osteoblasts (*10*). However, the exact mechanisms responsible for these changes remain elusive. One possible reason for these changes may be disruption of AChE signaling because bone marrow-derived MSCs express AChE, as demonstrated in literature (*10–12*). Another possibility is that OP compounds may have other unknown secondary effects (*13, 14*).

In the current study, we examined the signaling pathways associated with exposure to one of the most toxic OP CWAs, *O*-ethyl *S*-(2-diisopropylaminoethyl) methylphosphonothioate (VX), in an attempt to understand how these compounds affect MSCs.

1.2 MSCs

MSCs are multipotent adult stem cells that can be derived from several different types of tissues, including bone marrow, adipose tissue, dental pulp, and placenta (*15*). These cells typically have a limited differentiation capacity (e.g., osteoblasts, chondrocytes, and adipocytes) and play a significant role in tissue maintenance and repair (*15, 16*). MSCs have been shown to be capable of self-renewal and can be maintained in a multipotent state in vitro (*16*). Because no single marker is available to identify MSCs, the International Society for Cellular Therapy (ISCT; Vancouver, BC, Canada) published a consensus statement regarding identification requirements (*17*). In accordance with ISCT guidelines, MSCs must display the following properties:

- adherence to plastic under routine cell culture conditions;
- expression of the cluster of differentiation (CD) cellular markers, CD73, CD90, and CD105;

- lack of expression of CD11b, CD14, CD19, CD34, CD45, CD79a, and the human leukocyte antigen; and
- capacity for in vitro differentiation into osteoblasts, adipocytes, and chondrocytes.

1.3 OP Compounds

OP compounds were originally developed for use as powerful insecticides, but many of these compounds are too toxic for safe agricultural use. As a result of the elevated levels of toxicity that were observed during development, certain OP compounds were used as CWAs (*1, 2*). For example, the estimated human lethal concentration of VX that is lethal to 50% of the tested population (LCt_{50}) is 30–50 mg·min/m^3. In comparison, the well-known toxic agent, hydrogen cyanide has an estimated human LCt_{50} of 2860 mg·min/m^3 (*18*). OPs such as VX cause toxic effects by impacting the nervous system through the disruption of the normal action of AChE (*3, 4*). The main function of AChE is to terminate neural signal transmission through the degradation of the ACh neural transmitter molecule. When ACh degradation no longer occurs normally, it accumulates in the neural synapse and induces cholinergic hyperstimulation. In certain acute situations, this hyperstimulation can cause respiratory failure and eventual death. Although AChE is conventionally known for this signaling role in neurons, it has been speculated that it may also play a role in non-neural signaling. In fact, AChE has been shown to be expressed in several non-neuronal cell types including fibroblasts (*19*), megakaryocytes (*20*), erythrocytes (*21*), and endothelial cells (*22*). Studies have suggested that AChE may be involved in the regulation of cellular adhesion in non-neuronal cells (*19, 23–25*). It is possible that AChE may be acting in this capacity in MSCs, but further research will need to be performed to fully make this determination.

1.4 MSCs and OP Compounds

Deployed service members have the potential to be exposed to numerous toxic compounds, including OP-based CWAs and pesticides. These potential exposures could occur at low levels, which do not present any clinically measurable acute effects, and it is unclear whether these types of exposures carry a risk of long-term health effects such as heart, Alzheimer's, and Parkinson's diseases (*26–28*). In the literature, bone marrow-derived MSCs were shown to express active AChE, which affected the ability of MSCs to differentiate into osteoblasts and adipocytes (*10–12*). In a previous study, we demonstrated that parathion and its metabolite paraoxon reduced cellular viability and proliferative capability (*29*). We also demonstrated that exposure of the MSCs to either parathion or paraoxon had a direct impact on the activity and abundance of AChE in MSCs. Exposure to these OP compounds consequently reduced the adipogenic and osteogenic differentiation potential of MSCs (*29*).

2. MATERIALS AND METHODS

2.1 Human MSC Culture

Primary human bone marrow-derived MSCs were obtained from Lonza (Walkersville, MD) and cultured in MSC growth medium (MSCGM) that was supplemented with MSC growth supplement, L-glutamine, gentamicin, and amphotericin-B (medium and supplements were obtained from Lonza) (*10, 30, 31*). Cell culture medium was changed every 48–72 h, and the MSCs were subcultured after they achieved confluency in accordance with the manufacturer's recommended protocol. Only the MSCs from passages 5–8 were used in these studies.

2.2 Preparation of VX

The VX used in this study was synthesized and purified (≥90%) by ECBC team members from the Chemical Sciences Division in accordance with international regulations. Neat VX stocks were diluted into 1000 μg/mL (3.74 mM) working stocks with serum- and antibiotic-free cell culture medium.

2.3 Evaluation of VX-Induced Cell Morphology Changes

The MSCs were plated in 6-well tissue culture plates at a cellular density of 6×10^4 cells/well and allowed to attach overnight. The cells were then treated with 100 or 1000 μg/mL of VX or serum- and antibiotic-free media for 4 h. After the treatment, the MSCs were visualized with a Zeiss Axiovert 200 microscope (Carl Zeiss Microscopy, LLC, Thornwood, NY), and images were captured with a digital camera.

2.4 Evaluation of Cellular Impedance

Cellular impedance measurements were performed using the xCELLigence real-time cell analyzer (RTCA) system (ACEA Biosciences, Inc., San Diego, CA). Background impedance readings (i.e., with serum- and antibiotic-free media only, no cells) were taken before the start of an experiment. After the background readings, MSCs were plated in the wells of an E-Plate 96 Cardio device (Omni Life Science, East Taunton, MA), which is a single-use, disposable device used for performing cell-based assays on the RTCA Cardio instrument. The MSCs were plated at a density of 1×10^4 cells/well and allowed to attach overnight. Baseline impedance measurements were taken over a 1 h time period. The MSCs were then exposed to increasing concentrations of VX (1, 10, 100, or 1000 μg/mL) or to serum- and antibiotic-free media for 20 h. During the exposures, impedance readings were taken every 15 min and reported as a normalized cell index (CI), which was calculated in accordance with the xCELLigence system manufacturer's recommendations (*32*).

2.5 VX Exposure Procedures for Cell Lysate Collection

MSCs were grown to 80–90% confluence in T150 cell culture flasks (USA Scientific, Inc., Ocala, FL) and then serum-starved for approximately 2 h before exposure. After that, the cells were exposed to 100 μg/mL of VX for 5, 15, 30, or 60 min, and media-treated MSCs were used as controls. The VX concentration that was used was based on the impedance and morphology results. At each time point, the media was removed and the MSCs were washed four times with ice-cold, phosphate-buffered saline to remove any residual VX. Next, the cells were exposed to either the lysis buffer supplied with the Proteome Profiler Human Phospho-Kinase Array kit ARY003B (R&D Systems, Inc., Minneapolis, MN) or 4% sodium dodecyl sulfate in 100 mM Tris-HCl (pH 7.5), and then, they were scraped and collected. Finally, the samples were centrifuged at 14,000 rpm for 10 min at 4 °C, the supernatant was collected, and stored at –80 °C until use. The sample protein concentrations were determined using the Bicinchoninic acid assay (Thermo Fisher Scientific, Inc., Waltham, MA).

2.6 Phospho-Kinase Array Analysis

The Proteome Profiler Human Phospho-Kinase Array Kit was used to determine possible signaling cascades initiated in MSCs through exposure to VX. This assay is used to examine the activity of 46 types of intracellular signaling kinases. The assay was performed using the following steps in accordance with the manufacturer's recommendations:

(1) The membranes were blocked for 1 h at room temperature using the blocking reagent supplied with the kit.
(2) The membranes were incubated overnight with 235 μg of protein lysate at 4 °C.
(3) The membranes were rinsed with the washing buffer that was supplied and then exposed to secondary antibodies for 2 h at room temperature.
(4) The membranes were washed and treated with streptavidin–horseradish peroxidase solution and developed using the chemiluminescent reagent that was supplied.
(5) The signals were visualized using the Amersham Biosciences Typhoon 9400 Variable Mode Imager (GE Healthcare, Wauwatosa, WI).
(6) The images were evaluated for pixel intensity using ImageJ software (National Institutes of Health, Bethesda, MD).

2.7 Proteomic Analysis

2.7.1 Protein Digestion and Desalting

Protein samples were processed using the following modified filter-aided sample preparation procedure (*33*).

(1) Dithiothreitol was added to the samples for a final concentration of 10 mM for a total of 1 mg of protein and then the solution was boiled at 90 ºC with shaking for 15 min.

(2) The samples were diluted with 7 mL of UA buffer (8 M urea, 100 mM Tris-HCl, pH 8.6) and loaded onto an Ultra-15 mL, 10K molecular weight cut-off cellulose filter (EMD Millipore no. UFC901008).
(3) Each sample was centrifuged at 3220 G until the volume was reduced to approximately 100 µL (~30 min).
(4) Samples were alkylated on a filter by adding 100 µL of 0.05 M of iodoacetamide in UA buffer and incubated at room temperature in the dark for 30 min.
(5) After alkylation, the filters were washed three times with 2 mL of 100 mM triethylammonium bicarbonate (TEAB).
(6) Then, 10 µg of trypsin/lys C in 200 µL of 100 mM TEAB was added to the samples and allowed to digest overnight at 37 ºC with shaking.
(7) After incubation, the supernatant was spun through the column and retained for peptide quantitation.
(8) The filter was washed two times with 50 µL of 100 mM TEAB and one time with 0.5 M sodium chloride.
(9) The resultant washes were pooled with the original supernatant for subsequent peptide quantitation, and the pooled peptide supernatant was acidified to a final concentration of 1% formic acid using a glass syringe.
(10) Oasis HLB 1 cc (30 mg) reverse-phase cartridges (Waters Corporation, Milford, MA) were used to desalt each sample in accordance with the manufacturer's protocol.

2.7.2 Peptide Quantitation and Thermo Scientific Tandem Mass Tag (TMT) Labeling

Each sample was reconstituted with 1 mL of 30% acetonitrile and solubilized by vortexing for 10 min and sonicating for an additional 10 min. The peptides were quantified using the Pierce Quantitative Colorimetric Peptide Assay kit (Thermo Fisher Scientific) in accordance with the manufacturer's protocol. Each sample was labeled using ThermoFisher's 10 plex TMT system with some slight modifications.

(1) Each tag (5 mg) was resuspended in 256 µL of anhydrous acetonitrile, vortexed, and allowed to dissolve for 5 min at room temperature before use.
(2) Each sample was diluted with 100 mM TEAB to a final concentration of 0.7 µg/µL, and 700 µg (990 µL) of the dilution was mixed with 256 µL of a unique TMT and incubated at room temperature for 1 h.
(3) The reaction was quenched by adding 50% hydroxylamine to a final concentration of 0.7% for 15 min at room temperature.
(4) All of the samples were combined (five in total), dried to completeness, and stored at –80 °C.

2.7.3 Basic Reverse-Phase Liquid Chromatography (bRPLC)

TMT-labeled peptide mixtures were fractionated by bRPLC in the following manner (*34*):

- The sample was reconstituted in 3.6 mL of 20 mM ammonium formate/10% acetonitrile pH 10 (buffer A) and loaded by syringe pump onto a Waters XBridge C18, 5 µm, 4.6 × 250 mm column with a Waters XBridge C18, 5 µm, 4.6 × 20 mm guard cartridge.
- The column was then connected to an Agilent 1260 high-performance liquid chromatography pump system (Santa Clara, CA) that was equipped with an analytical scale fraction collector.
- The flow rate was set to 200 µL/min. Buffer A comprised 20 mM of ammonium formate/10% acetonitrile pH 10, and Buffer B comprised 20 mM of ammonium formate/90% acetonitrile pH 10.

The peptides were separated using the gradient shown in Table 1.

Table 1. Basic Reverse-Phase Peptide Fractionation Gradient

Gradient	
Time (min)	Buffer B (%)
0–5	0
5–13	0–15
13–46	15–28.5
46–51.5	28.5–34
51.5–64.5	34–60

The first 5.5 min were pooled into a single "Early" fraction and the final 9.2 min were pooled into a single "Late" fraction. Between the Early and Late fractions, 84 single fractions were collected every 0.6 min. These 84 fractions were pooled in accordance with the early, mid, and late concatenation strategy for a total of 14 fractions (*35*). The fractions were acidified with 200 µL of 10% formic acid, split into two aliquots (90% for phosphopeptide enrichment and 10% for total proteome analysis), and dried to completeness. Phosphopeptides were enriched using the TiO Enrichment Kit (Thermo Fisher Scientific; Pierce #90003) in accordance with the manufacturer's instructions.

2.7.4 Liquid Chromatography–Mass Spectrometry Analysis (LC–MS)

Immediately before LC–MS analysis was performed, each fraction was reconstituted in 20 µL of 5% formic acid/5% acetonitrile and vortexed for 5 min at room temperature to completely dissolve the sample. Each fraction was analyzed on a ThermoFisher Orbitrap Q Exactive Plus mass spectrometer coupled with a ThermoScientific UltiMate 3000 nano rapid separation LC system. Injections of each sample (2 µL) were first preconcentrated on a ThermoFisher reverse-phase trapping column (PepMap 300 C18LC column; length: 5 mm; ID: 300 µm; 100 Å particles) and then resolved on a 75 µm × 500 mm

Thermo Fisher EASY-Spray column packed with PepMap LC, C18, 2 μm, 100 Å particles using a 182 min multistep gradient (Table 2) (*34*).

Table 2. Online LC–MS Gradient

Gradient	
Time (min)	Buffer B Hold (%)
0–150	6–35
150–158	35–60%
158–161	60–90
161–171	90
171–172	90–6
172–182	6

For the gradient, Buffer A comprised 100% water/0.1% formic acid and Buffer B comprised 80% acetonitrile/0.1% formic acid. Orbitrap MS1 scans were performed at a resolution of 70,000 at 400 mass-to-charge ratio (m/z), with a scan range of 300–1700 m/z in profile mode. The top 12 precursors were selected for tandem mass spectrometry (MS2) data-dependent fragmentation. MS2 spectra was acquired in centroid mode with a resolution of 35,000 in the Orbitrap spectrometer with the first mass fixed to 100 m/z to capture TMT report ions. The minimum signal required to trigger a data-dependent scan was 8000 with an underfill ratio of 1%. Peptide match was set to "preferred"; exclude isotopes was set to "on"; and charge exclusion was set to "unassigned, 1, 8, >8". Higher-energy, C-trap dissociation was used to generate MS2 spectra with the following settings: stepped normalized collision energy at 26% and isolation width of 2 m/z. The automatic gain control target was set to 3 × 106 for MS and 1 × 105 for MS2 with a maximum accumulation time of 120 ms. Dynamic exclusion was set at 20 s with a 5 ppm mass window.

2.7.5 MS Data Analysis

Spectra data were processed using Proteome Discoverer 2.1 with the Sequest HT search algorithm against the National Center for Biotechnology Information (Bethesda, MD) refseq database for Homo sapiens. Dynamic modifications were set for the oxidation of methionine [+15.99 Da]; phosphorylation of serine, threonine, and tyrosine [+79.966]; and N-terminal acetylation [+42.011]. Static modifications were set to carbamidomethylation of cysteine [+57.02 Da], N-terminal TMT 6 plex [+229.16 Da], and TMT labeling of lysine [+229.16 Da]. MS2 spectra were searched with a precursor mass tolerance of 10 ppm and a fragment mass tolerance of 0.02 Da. Trypsin was specified as the protease with a maximum number of missed cleavages set to 2. A false discovery rate was calculated using the Percolator algorithm, which was set at <1% to score high-confidence peptide identifications. Protein relative quantification was calculated using intensity ratios of TMT reporter ions. Statistical and enrichment analyses were performed using Perseus software (Microtelecom s.r.l., Pavia di Udine, Italy).

3. RESULTS

3.1 Effect of VX on Cellular Impedance

The MSCs were treated with increasing concentrations of VX (1–1000 µg/mL) or with media only for 20 h. These exposures induced a dose-dependent decrease in normalized CI values (Figure 1). Within 30 min of the initial exposure, normalized CI values significantly decreased at all of the VX dose levels examined. These values continued to decrease throughout the duration of the experiment (20 h).

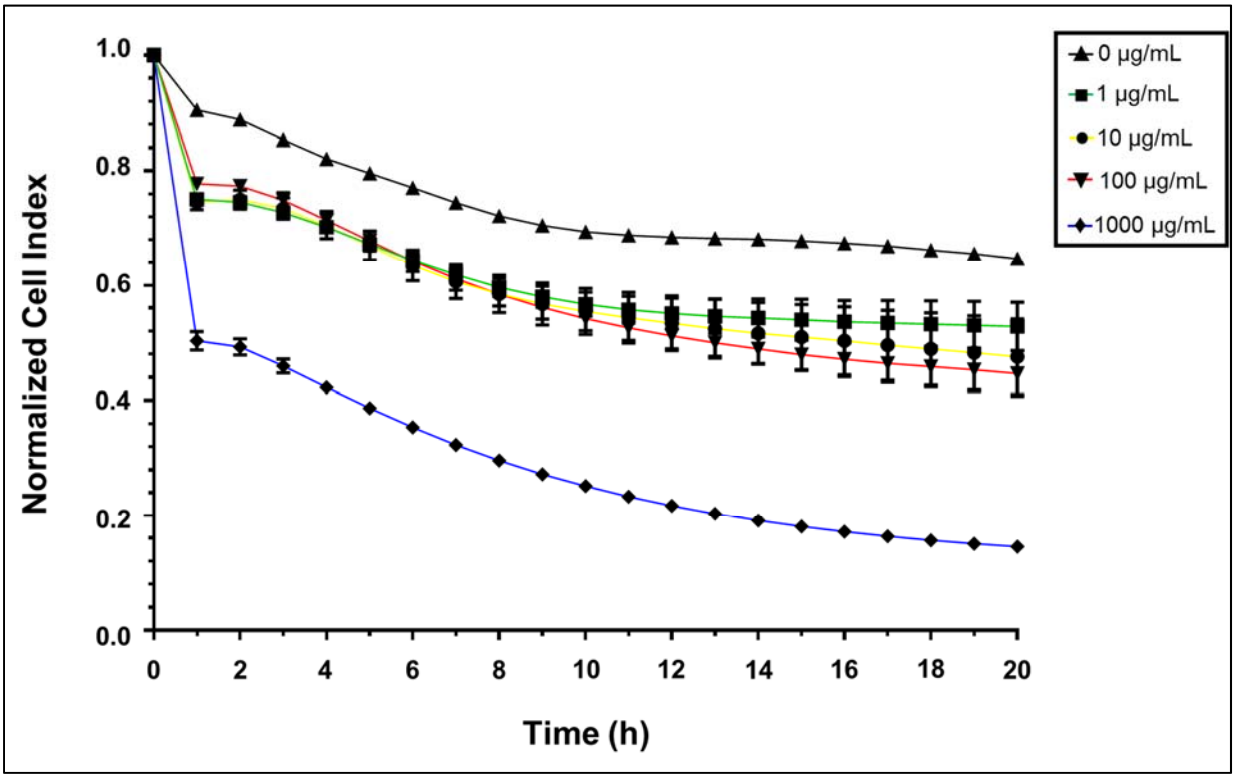

Figure 1. Cellular impedance changes in cultured MSCs following VX exposure. MSCs were exposed to increasing concentrations of VX (1, 10, 100, or 1000 µg/mL) or to media only for 20 h. The results are expressed as the mean ± standard error of the mean of the normalized CI (i.e., $n \geq 8$ for each experimental condition). ▲ (Black) media control, ■ (green) 1 µg/mL of VX, ● (yellow) 10 µg/mL of VX, ▼ (red) 100 µg/mL of VX, and ♦ (blue) 1000 µg/mL of VX.

3.2 Morphological Changes Associated with VX Exposure

MSCs were cultured in 6-well tissue culture dishes and treated with 100 or 1000 µg/mL of VX or with media only for 4 h (Figure 2). The experimental doses were determined from the initial cellular impedance experiments. After treatment, the MSCs exposed to VX (Figure 2D–I) displayed distinct morphological changes compared with the MSCs exposed to media only (Figure 2A–C). The MSCs treated with the 1000 µg/mL VX started to

shrink and peel off from the extracellular matrix within 30 min of exposure and continued with these alterations for 4 h (Figure 2G-I). The 100 µg/mL of VX exposures also sustained similar morphological changes but to a lesser extent (Figure 2D–F).

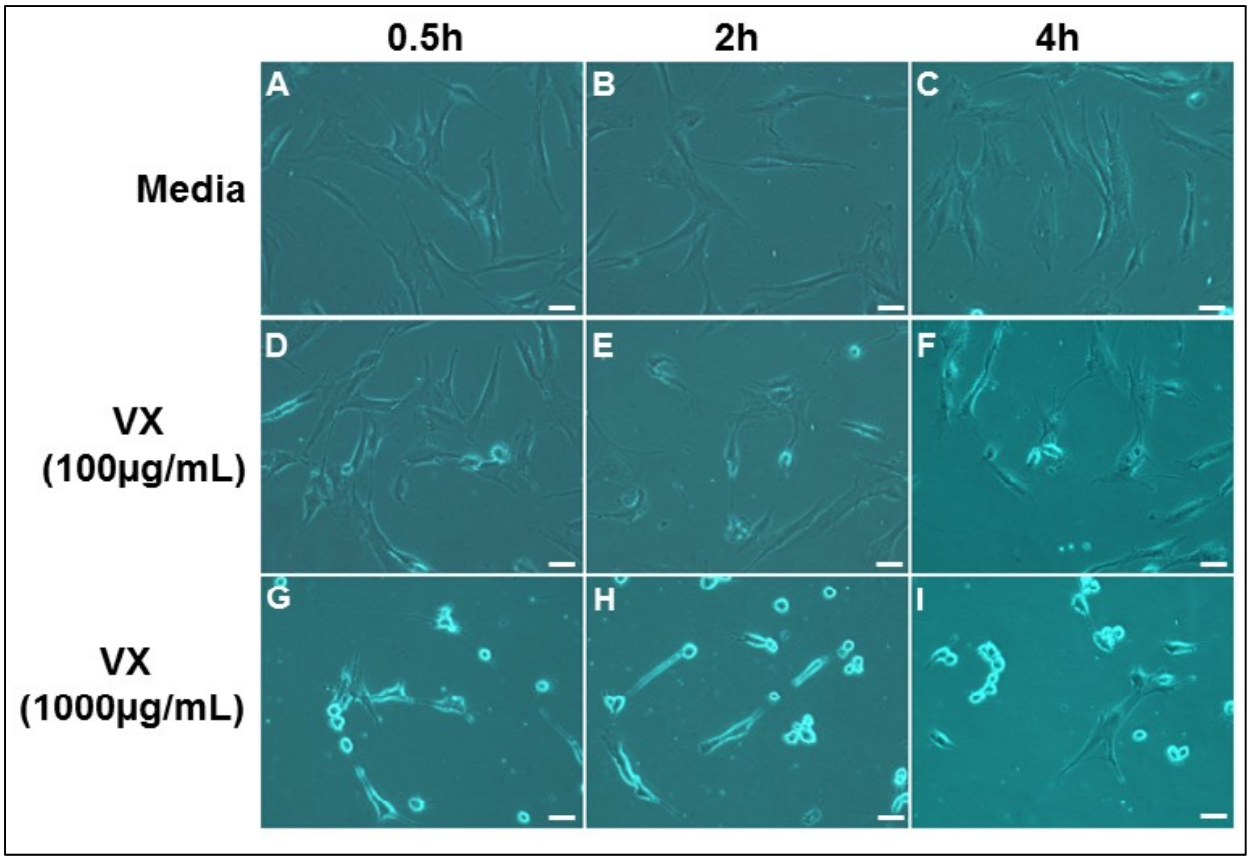

Figure 2. Morphological changes in cultured MSCs following VX exposure. Phase contrast images of MSCs exposed to (A–C) media, (D–F) 100 µg/mL of VX, or (G–I) 1000 µg/mL of VX for 0.5, 2, and 4 h. Bar = 100 µm.

3.3 VX-Induced Changes in Protein Expression

Cultured MSCs were exposed to media or VX (100 µg/mL) for 5, 15, 30, or 60 min. This VX concentration was based on the results of the impedance and morphology experiments. The cells were processed for proteomic analysis, as described in Section 2.7.4. Table 3 displays the abundance ratio of proteins that showed at least a 2.5-fold increase or decrease at 60 min of VX exposure. This analysis identified 12 such proteins. Ten of the proteins demonstrated at least a 2.5-fold increase in protein expression and two displayed at least a 2.5-fold decrease in protein expression. The protein with the greatest increase (~5.8-fold) after exposure to VX was Thy-1 or CD90. This protein was one of the markers used for the identification of MSCs (*17*). Thy-1 functions have not been fully identified, but it has been suggested that the protein may play a role in several different processes, including cognition, axon growth regulation, cellular adhesion, and regulating apoptosis or necrosis (*36–39*). Another protein of note that was increased more than 2.5-fold was macrophage migration inhibitor factor

(MIF). The protein is classified as an inflammatory cytokine and regulator of innate immunity (*40*, *41*); clinically, this cytokine plays a role in sepsis and rheumatoid arthritis.

Table 3. Protein Expression Change following 60 min VX Exposure

	Protein Name	Gene Symbol	Abundance Ratio
1	Thy-1 membrane glycoprotein preproprotein	THY1	5.781
2	Fibronectin isoform 5 preproprotein	FN1	3.627
3	Histone H2A.x	H2AX	3.588
4	ATP synthase subunit gamma, mitochondrial isoform L (liver) precursor	ATP5C1	3.432
5	Rho-related GTP-binding protein RhoC precursor	RHOC	3.386
6	Histone H2A type 2-A	HIST2H2AA3	3.179
7	Macrophage migration inhibitory factor	MIF	2.652
8	DNA polymerase Δ catalytic subunit	POLD1	2.592
9	Histone H2B Type 2-F isoform β	HIST2H2BF	2.516
10	Hemoglobin subunit α	HBA1	2.511
11	Leucine-rich repeat-containing protein	LRRC41	0.386
12	HBS1-like protein isoform 3	HBS1L	0.220

ATP: adenosine triphosphate
GTP: guanosine 5'-triphosphate

3.4 VX-Induced Signaling Pathway Activation

MSCs were exposed to media or VX (100 µg/mL) for 15 or 30 min. Our phospho-array results demonstrated phosphorylation changes in five different proteins (Figure 3). VX induced an increase in the phosphorylation state of extracellular signal-regulated kinases 1/2 (ERK1/2) by approximately 3.4-fold and proline-rich Akt substrate of 40 kDa (PRAS40) by approximately 1.9-fold after 15 min of exposure. After 30 min of exposure, the phosphorylation state appeared to be returning to baseline: 1.5-fold for ERK1/2 and 1.2-fold for PRAS40. Both of these proteins are known to affect cell survival signaling; ERK1/2 is involved in signaling associated with cell proliferation, differentiation, and survival (*42*), and PRAS40 is involved in the Akt signaling pathway and is associated with cell survival and cancer (*43*). Three other proteins appeared to be dephosphorylated after exposure to VX; these proteins included heat shock protein 27 (HSP27), glycogen synthase kinase 3 alpha/beta (GSK3α/β), and WNK lysine deficient protein kinase 1 (WNK1). These proteins have been shown to act as either negative regulators of apoptosis or regulators of the actin cytoskeleton (*44–46*).

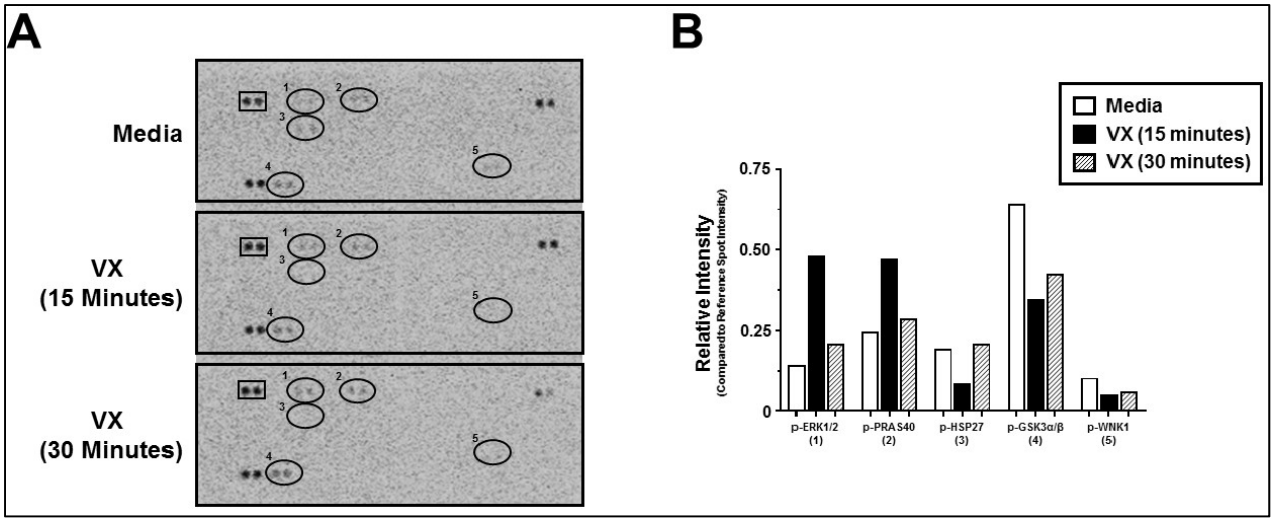

Figure 3. Phospho-array analysis of VX-exposed MSCs. (A) Phospho (p)-array membranes were incubated with 225 µg of cellular lysate from MSCs exposed to media or VX (100 µg/mL) for 15 or 30 min. Ovals represent spots that change over time (1) p-ERK1/2, (2) p-PRAS40, (3) p-HSP27, (4) p-GSK3α/β, and (5) p-WNK1. (B) Relative intensity of pixels were compared with the reference spots (within rectangles) using ImageJ software.

3.5 Phosphoproteomic Analysis

MSCs were exposed to media or VX (100 µg/mL) for 5, 15, 30, or 60 min. The treated cells were collected and processed for proteomic analysis. Figure 4A shows the global heat map indicating the overall increases (red) and decreases (green) in the protein phosphorylation states. There appears to be some slight changes in overall phosphorylation at 5 min post-exposure, but the major phosphorylation changes (increases and decreases) seem to appear at the 60 min time point. For this study, proteins that exhibited a 2-fold increase or decrease in phosphorylation levels were considered significant. These results demonstrated phosphorylation changes in six different proteins after exposure to VX (Figure 4B). Three proteins displayed increased phosphorylation, including PEST proteolytic signal-containing nuclear protein (PCNP); regulating synaptic membrane exocytosis protein 1 isoform 2 (RIMS1); and 1-phosphatidylinositol-4,5-bisphosphate phosphodiesterase γ-1 isoform α (PLCG1). PCNP has been shown to be involved in the regulation of cell proliferation (*47*). RIMS1, also known as Rab3-interacting molecule, regulates synaptic vesicle exocytosis and is a member of the Ras superfamily (*48*). PLCG1 has been shown to play a role in cell migration and invasion in cancer cells (*49*) and can be activated in response to *Yersinia pseudotuberculosis* infection (*50*). Three proteins were shown to be dephosphorylated at least 2-fold after VX exposure. These proteins include FARP2 (FERM, RhoGEF, and pleckstrin domain-containing protein 2), YAF2 (YY1-associated factor 2 isoform 1), and RPAP1 (ribonucleic acid [RNA] polymerase II-associated protein 1). FARP2 is involved in podosome rearrangements in osteoclasts (*51*). YAF2 has been shown to inhibit caspase-mediated apoptosis during zebrafish development (*52*). RPAP1 is involved in the regulation of certain aspects of DNA binding and transcription (*53*).

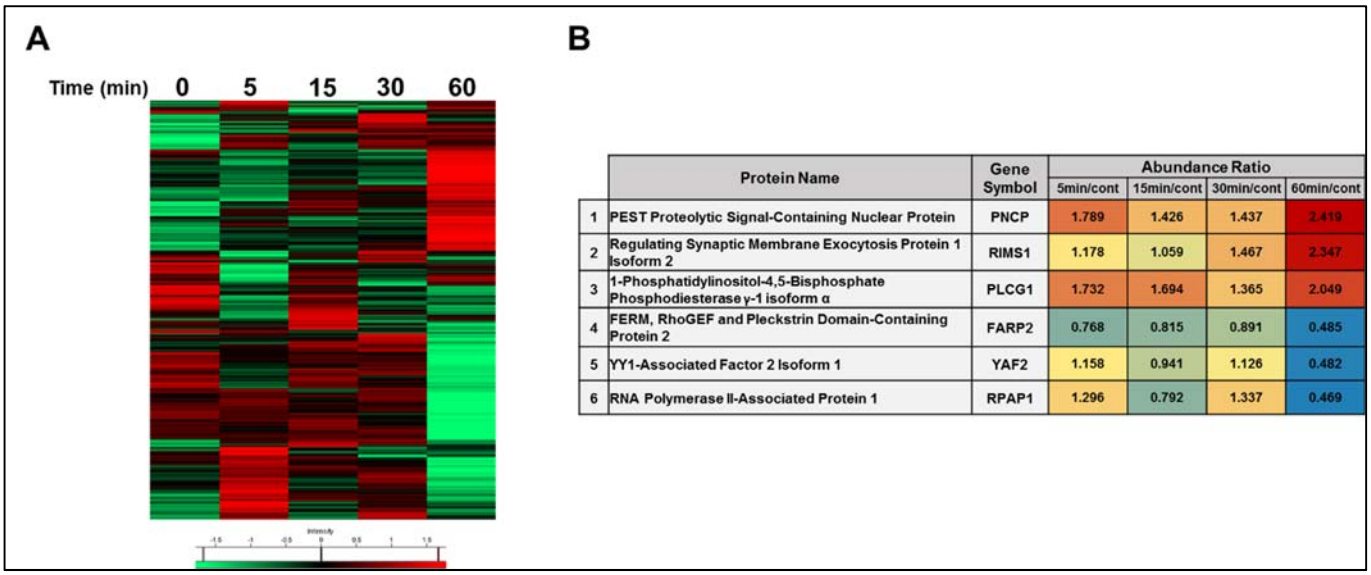

	Protein Name	Gene Symbol	Abundance Ratio			
			5min/cont	15min/cont	30min/cont	60min/cont
1	PEST Proteolytic Signal-Containing Nuclear Protein	PNCP	1.789	1.426	1.437	2.419
2	Regulating Synaptic Membrane Exocytosis Protein 1 Isoform 2	RIMS1	1.178	1.059	1.467	2.347
3	1-Phosphatidylinositol-4,5-Bisphosphate Phosphodiesterase γ-1 isoform α	PLCG1	1.732	1.694	1.365	2.049
4	FERM, RhoGEF and Pleckstrin Domain-Containing Protein 2	FARP2	0.768	0.815	0.891	0.485
5	YY1-Associated Factor 2 Isoform 1	YAF2	1.158	0.941	1.126	0.482
6	RNA Polymerase II-Associated Protein 1	RPAP1	1.296	0.792	1.337	0.469

Figure 4. Phosphoproteomic analysis of VX-exposed MSCs. (A) Heat map of the phosphorylation state of analyzed proteins. Red indicates an increase in the phosphorylation state and green indicates a reduction in the phosphorylation state. (B) List of the proteins that displayed either a 2-fold increase or 2-fold decrease in phosphorylation levels.

3.6 Phospho-Peptide Analysis

In addition to the phospho-protein analysis, we performed a more detailed phospho-peptide analysis on VX-exposed MSCs. A different set of peptides was generated from this analysis. Eight peptides displayed at least a 2-fold increase in phosphorylation in response to VX exposure, compared with the untreated control (Table 4). Of the phosphorylated peptides, WD repeat-containing protein 6 (WDR6) displayed the greatest phospho-peptide increase. WDR6 reached its peak phosphorylation state at 15 min post-exposure to VX with a 4.19-fold increase. This protein is associated with cell cycle arrest and negative regulation of cellular proliferation (*54*). The other phosphorylated peptides were associated with various cellular functions. Disks large-associated protein 4 (DLGAP4) has been associated with neuronal cell signaling and the organization of synapses in nervous tissue (*55*). The mRNA decay activator protein (ZFP36) is RNA-binding and has been implicated in the mRNA decay process (*56*). Heterogeneous nuclear ribonucleoprotein A0 (hnRNP A0) is also an RNA-binding protein that has been shown to be highly expressed in hematopoietic stem cells (*57*). Vimentin (VIM) is involved in intermediate filament organization, especially in MSCs (*58*). The multiprotein complex, 26S proteasome non-ATPase regulator subunit 11 (PSMD11), is involved in the ATP-dependent degradation of ubiquitinated proteins (*59*). Phosphorylase b kinase regulator subunit beta (PHKB) has been shown to be involved in the breakdown of glycogen (*60*). Finally, protein kinase C (PRKC) apoptosis WT1 regulator protein (PAWR) is involved in regulating the actin cytoskeleton and the apoptotic signaling pathway (*61*).

Table 4. Phospho-Peptide Increases following 60 min VX Exposure

	Protein Name	Gene Symbol	Peptide Sequence	Phosphosite on Peptide	Phosphosite on Protein	Abundance Ratio			
						5min	15min	30min	60min
1	Disks Large-Associated Protein 4	DLGAP4	SEVTSQSGLSNSSDSLDSSTRPP**S**VRT	(S24)	(S620)	2.582	1.062	1.752	0.521
2	WD Repeat-Containing Protein 6	WDR6	GLLATASEDR**S**VR	(S11)	(S232)	2.383	4.19	3.248	2.89
3	mRNA Decay Activator Protein ZFP36	ZFP36	ST**S**LVEGR	S3	S60	2.333	1.17	1.999	1.831
4	Vimentin	VIM	LR**S**SVPGVR	S3	S72	2.253	1.41	2.279	1.552
5	26S Proteosome Non-ATPase Regulatory Subunit 11	PSMD11	AQ**S**LSTDR	S3	S14	2.186	1.189	1.742	1.157
6	Heterogeneous Nuclear Ribonucleoprotein A0	HNRNPA0	AV**S**REDSARPGAHAK	S3	S84	2.11	0.748	1.683	1.302
7	Phosphorylase b Kinase Regulatory Subunit β	PHKB	SG**S**VYEPLK	S3	S27	2.081	1.218	1.826	1.706
8	PRKC Apoptosis WT1 Regulator Protein	PAWR	R**S**TGVVNIPAAECLDEYEDDEAGQK	(S2)	(S162)	2.027	1.59	2.332	1.816

Note: The phosphorylation site is indicated in red.
( ): Assignment of phosphorylation site(s) is ambiguous.
The site in parenthesis is the top-ranked candidate.

The following 14 peptides were identified. These were dephosphorylated at least 2-fold in response to VX exposure, as compared with the untreated controls:

- Vinculin (VCL) is a protein that is involved in linking adherens junctions and focal adhesions to the actin cytoskeleton (*62*). In addition, VCL has been shown to associate with AChE in MSCs, and this association may be affected by OP exposure (*29*).
- Filaggrin (FLG) is an intermediate filament protein that has been shown to be involved in the structure of the epidermis and skin barrier (*63*). Upregulation of filaggrin in keratinocytes has been associated with susceptibility to apoptosis (*64*).
- C-type mannose receptor 2 (MRC2) is associated with osteoblast differentiation (*65*). In a previous study, we demonstrated that exposing MSCs to OP pesticides reduces the potential for these cells to differentiate into bone (*29*); it is possible that this dephosphorylation event may be involved in this process.
- Transient receptor potential cation channel subfamily M member 7 (TRPM7) is involved in the regulation of Ca^{2+} and Mg^{2+} homeostasis, and alterations in this protein have been implicated in neurodegenerative disorders (*66*). Recent studies have suggested that TRPM7 plays a regulatory role in cell proliferation, cell survival, and cytoskeletal organization (*67*).
- SH3 and PX domain-containing protein 2A (SH3PXD2A; also known as Fish, Tks5, and SH3MD1) is a scaffold protein associated with the formation of podosomes or invadopodia (*68*). Src homology 3 domain-containing kinase-binding protein 1 (SH3KBP1; also known as CIN85) is an adaptor protein associated with the actin cytoskeleton and downregulation and degradation of receptor tyrosine kinases (*69*).
- Bifunctional glutamate/proline–tRNA ligase (EPRS) and eukaryotic translation initiation factor 4G (EIF4G1) are potential binding partners that are involved in RNA processing and translation (*70*).
- La-related protein 7 (LARP7) has been shown to be a negative regulator of polymerase II genes (*71*).
- Tumor protein D54 (TPD52L2) is involved in the regulation of cellular attachment and migration (*72*).
- Calnexin (CANX) is associated with regulation of protein-folding (*73*) and FERM, RhoGEF, and pleckstrin domain-containing protein 1 (FARP1) is associated with dendrite morphogenesis and Rho signal transduction (*74*).

Many of the peptides that were altered in response to VX are associated with the cytoskeleton or the regulation of the cell cycle/apoptosis. This may explain the reductions in cellular impedance and changes in morphology observed in response to VX treatment (Table 5).

Table 5. Phospho-Peptide Decreases following 60 min VX Exposure

	Protein Name	Gene Symbol	Peptide Sequence	Phosphosite on Peptide	Phosphosite on Protein	Abundance Ratio			
						5min	15min	30min	60min
1	C-type mannose receptor 2	MRC2	YSRSSSSPTEATEK	(S4, S5)	(S1455, S1456)	0.31	0.936	0.683	0.603
2	Filaggrin	FLG	QSGTPHAETS**S**GGQAASSHEQARSSPGER	(S11)	(S1014)	0.362	0.609	0.644	0.141
3	Eukaryotic translation initiation factor 4 γ, 3 variant	N/A	GG**S**SKDLLDNQSQEEQRR	S3	S1351	0.378	0.64	0.416	0.326
4	SH3 domain-containing kinase-binding protein 1	SH3KBP1	SSLRETTGSE**S**DGGDSSSTK	S11	S183	0.428	0.86	0.807	0.469
5	Vinculin	VCL	ARGQGS**S**PVAMQK	S7	S346	0.454	0.965	0.673	1.405
6	Transient receptor potential cation channel subfamily M member 7	TRPM7	I**S**RRP**S**TEDTHEVDSK	S2, S6	S1500, S1504	0.465	0.866	0.866	1.103
7	Calnexin	CANX	LEEKQK**S**DAEEDGGTVSQEEEDR	S7	S589	0.47	0.87	0.847	0.566
8	Tumor protein D54	TPD52L2	NSATFK**S**FEDR	S7	S189	0.476	0.772	0.331	0.393
9	EIF4G1 variant protein	EIF4G1 variant protein	**S**RERPSQPEGLRK	S1	S1219	0.484	0.825	0.469	0.315
10	Bifunctional glutamate/proline--tRNA ligase	EPRS	EYIPGQPPLSQSSD**S**SPTRNSEPAGLETPEAK	(S15)	(S885)	0.485	0.883	0.967	0.43
11	SH3 and PX domain-containing protein 2A	SH3PXD2A	RPAQPHRP**S**PA**S**SLQR	S9, S12	S593, S596	0.487	0.774	0.68	0.705
12	La-related protein 7	LARP7	RSRPT**S**EGSDIESTEPQK	(S6)	(S258)	0.488	0.748	0.512	0.396
13	FERM, RhoGEF and pleckstrin domain-containing protein 1	FARP1	VSAGEPGSHP**S**PAPRR**S**PAGNK	S11, S17	S427, S433	0.494	0.71	0.49	0.344

Note: The phosphorylation site is indicated in red.
( ): Assignment of phosphorylation site(s) is ambiguous.
The site in parenthesis is the top-ranked candidate.

4. CONCLUSIONS

Our results indicate that exposure to VX induces a drop in MSC cellular impedance in dose- and time-dependent manners. This change in impedance after VX exposure is in conjunction with alterations in MSC morphology. In our study, MSCs treated with 1000 μg/mL of VX started to shrink and peel off the extracellular matrix within 30 min of exposure; this process continued in the later time point (4 h). Lower concentrations of VX (100 μg/mL) also induced similar morphological changes but to a lesser extent. The phospho-array study revealed changes in five different proteins that changed phosphorylation state as a result of exposure to 100 μg/mL of VX: ERK1/2 and PRAS40 displayed increased phosphorylation, while HSP27, GSK3α/β, and WNK1 were dephosphorylated. These proteins are known to be involved in the regulation of cell survival or apoptosis. The phosphoproteomic analysis revealed significant changes in seven different proteins after VX exposure, including the phosphorylation of PCNP, PLCG1, and RIMS1 as well as the dephosphorylation of FARP2, YAF2, and RPAP1. These proteins appear to be involved in either intracellular signal regulation, cell cycle regulation, or cellular migration.

More detailed analyses of phospho-peptides revealed increases in the phosphorylation states of 8 peptides and decreases in 14 of them. The peptides that displayed at least 2-fold increases in phosphorylation included DLGAP4, WDR6, ZFP36, VIM, PSMD11, hnRNP A0, PHKB, and PAWR. The 14 peptides that were dephosphorylated at least 2-fold in response to VX exposure included MRC2, FLG, SH3KBP1, VCL, TRPM7, CANX, TPD52L2, EIF4G1 variant protein, EPRS, SH3PXD2A, LARP7, and FARP1. The functions of the proteins that contained these peptides were involved in cell-cycle regulation, apoptosis, and cytoskeleton regulation. Overall, this study has identified several previously unknown signaling pathways that are associated with low-level VX exposure in MSCs.

LITERATURE CITATIONS

1. Angelini, D.J.; Dorsey, R.M.; Willis, K.L.; Hong, C.; Moyer, R.A.; Oyler, J.; Jensen, N.S.; Salem, H. Chemical Warfare Agent and Biological Toxin-Induced Pulmonary Toxicity: Could Stem Cells Provide Potential Therapies? *Inhal. Toxicol.* **2013,** *25*, 37–62.

2. Sidell, F.R.; Borak, J. Chemical Warfare Agents: II. Nerve Agents. *Ann. Emerg. Med.* **1992,** *21*, 865–871.

3. Pohanka, M. Cholinesterases, a Target of Pharmacology and Toxicology. *Biomed. Pap. Med. Fac. Univ. Palacky Olomouc Czech Repub.* **2011,** *155*, 219–229.

4. Colovic, M.B.; Krstic, D.Z.; Lazarevic-Pasti, T.D.; Bondzic, A.M.; Vasic, V.M. Acetylcholinesterase Inhibitors: Pharmacology and Toxicology. *Curr. Neuropharmacol.* **2013,** *11*, 315–335.

5. Nambiar, M.P.; Gordon, R.K.; Rezk, P.E.; Katos, A.M.; Wajda, N.A.; Moran, T.S.; Steele, K.E.; Doctor, B.P.; Sciuto, A.M. Medical Countermeasure against Respiratory Toxicity and Acute Lung Injury following Inhalation Exposure to Chemical Warfare Nerve Agent VX. *Toxicol. Appl. Pharmacol.* **2007,** *219*, 142–150.

6. Rezk, P.E.; Graham, J.R.; Moran, T.S.; Gordon, R.K.; Sciuto, A.M.; Doctor, B.P.; Nambiar, M.P. Acute Toxic Effects of Nerve Agent VX on Respiratory Dynamics and Functions following Microinsillation Inhalation Exposure in Guinea Pigs. *Inhal. Toxicol.* **2007,** *19*, 291–302.

7. Lee, F.Y.; Chen, W.K.; Lin, C.L.; Lai, C.Y.; Wu, Y.S.; Lin, I.C.; Kao, C.H. Organophosphate Poisoning and Subsequent Acute Kidney Injury Risk: A Nationwide Population-Based Cohort Study. *Medicine (Baltimore)* **2015,** *94*, e2107.

8. Katos, A.M.; Conti, M.L.; Moran; T.S.; Gordon, R.K.; Doctor, B.P.; Sciuto, A.M.; Nambiar, M.P. Abdominal Bloating and Irritable Bowel Syndrome Like Symptoms following Microinstillation Inhalation Exposure to Chemical Warfare Nerve Agent VX in Guinea Pigs. *Toxicol. Ind. Health* **2007,** *23*, 231–240.

9. Collombet, J.M.; Mourcin, F.; Grenier, N.; Four, E.; Masqueliez, C.; Baubichon, D.; Lallement, G.; Herodin, F. Effect of Soman Poisoning on Populations of Bone Marrow and Peripheral Blood Cells in Mice. *Neurotoxicology* **2005,** *26*, 89–98.

10. Prugh, A.M.; Cole, S.D.; Glaros, T.; Angelini, D.J. Effects of Organophosphates on the Regulation of Mesenchymal Stem Cell Proliferation and Differentiation. *Chem. Biol. Interact.* **2017,** *266*, 38–46.

11. Hoogduijn, M.J.; Cheng, A.; Genever, P.G. Functional Nicotinic and Muscarinic Receptors on Mesenchymal Stem Cells. *Stem Cells Dev.* **2009,** *18*, 103–112.

12. Hoogduijn, M.J.; Rakonczay, Z.; Genever, P.G. The Effects of Anticholinergic Insecticides on Human Mesenchymal Stem Cells. *Toxicol. Sci.* **2006,** *94*, 342–350.

13. Carmany, D.; Walz, A.J.; Hsu, F.L.; Benton, B.J.; Burnett, D.; Gibbons, J.A.; Noort, D.; Glaros, T.G.; Sekowski, J.W. Activity Based Protein Profiling Leads to Identification of Novel Protein Targets for the Nerve Agent VX. *Chem. Res. Toxicol.* **2017,** *30*(4), 1076–1084.

14. Nirujogi, R.S.; Wright, J.D., Jr.; Manda, S.S.; Zhong, J.; Na, C.H.; Meyerhoff, J.; Benton, B.; Jabbour, R.; Willis, K.; Kim, M.S.; Pandey, A.; Sekowski, J.W. Phosphoproteomic Analysis Reveals Compensatory Effects in the Piriform Cortex of VX Nerve Agent Exposed Rats. *Proteomics* **2015,** *15*, 487–499.

15. Rastegar, F.; Shenaq, D.; Huang. J.; Zhang, W.; Zhang, B.Q.; He, B.C.; Chen, L.; Zuo, G.W.; Luo, Q.; Shi, Q.; Wagner, E.R.; Huang, E.; Gao, Y.; Gao, J.L.; Kim, S.H.; Zhou, J.Z.; Bi, Y.; Su, Y.; Zhu, G.; Luo, J.; Luo, X.; Qin, J.; Reid, R.R.; Luu, H.H.; Haydon, R.C.; Deng, Z.L.; He, T.C. Mesenchymal Stem Cells: Molecular Characteristics and Clinical Applications. *World J. Stem Cells* **2010,** *2*, 67–80.

16. Pittenger, M.F.; Mackay, A.M.; Beck, S.C.; Jaiswal, R.K.; Douglas, R.; Mosca, J.D.; Moorman, M.A.; Simonetti, D.W.; Craig, S.; Marshak, D.R. Multilineage Potential of Adult Human Mesenchymal Stem Cells. *Science* **1999,** *284*, 143–147.

17. Dominici, M.; Le Blanc, K.; Mueller, I.; Slaper-Cortenbach, I.; Marini, F.; Krause, D.; Deans, R.; Keating, A.; Prockop, D.; Horwitz, E. Minimal Criteria for Defining Multipotent Mesenchymal Stromal Cells. The International Society for Cellular Therapy Position Statement. *Cytotherapy* **2006,** *8*, 315–317.

18. *Defense USAMRIoC: Medical Management of Chemical Casualties Handbook*. 4th ed; U.S. Government Printing Office: Washington, DC, 2007.

19. Anderson, A.A.; Ushakov, D.S.; Ferenczi, M.A.; Mori, R.; Martin, P.; Saffell, J.L. Morphoregulation by Acetylcholinesterase in Fibroblasts and Astrocytes. *J. Cell. Physiol.* **2008,** *215*, 82–100.

20. Paulus, J.M.; Maigne, J.; Keyhani, E. Mouse Megakaryocytes Secrete Acetylcholinesterase. *Blood* **1981,** *58*, 1100–1106.

21. Herz, F.; Kaplan, E. A Review: Human Erythrocyte Acetylcholinesterase. *Pediatr. Res*. **1973,** *7*, 204–214.

22. Carvalho, F.A.; Graca, L.M.; Martins-Silva, J.; Saldanha, C. Biochemical Characterization of Human Umbilical Vein Endothelial Cell Membrane Bound Acetylcholinesterase. *FEBS J*. **2005,** 272, 5584–5594.

23. Bigbee, J.W.; Sharma, K.V. The Adhesive Role of Acetylcholinesterase (AChE): Detection of AChE Binding Proteins in Developing Rat Spinal Cord. *Neurochem. Res.* **2004,** *29*, 2043–2050.

24. Paraoanu, L.E.; Layer, P.G. Acetylcholinesterase in Cell Adhesion, Neurite Growth and Network Formation. *FEBS J*. **2008,** *275*, 618–624.

25. Sharma, K.V.; Bigbee, J.W. Acetylcholinesterase Antibody Treatment Results in Neurite Detachment and Reduced Outgrowth from Cultured Neurons: Further Evidence for a Cell Adhesive Role for Neuronal Acetylcholinesterase. *J. Neurosci. Res.* **1998,** *53*, 454–464.

26. Rocksen, D.; Elfsmark, D.; Heldestad, V.; Wallgren, K.; Cassel, G.; Goransson Nyberg, A. An Animal Model to Study Health Effects during Continuous Low-Dose Exposure to the Nerve Agent VX. *Toxicology* **2008,** *250*, 32–38.

27. Terry, A.V., Jr. Functional Consequences of Repeated Organophosphate Exposure: Potential Non-Cholinergic Mechanisms. *Pharmacol. Ther.* **2012,** *134*, 355–365.

28. Wang, A.; Cockburn, M.; Ly, T.T.; Bronstein, J.M.; Ritz, B. The Association between Ambient Exposure to Organophosphates and Parkinson's Disease Risk. *Occup. Environ. Med.* **2014,** *71*, 275–281.

29. Prugh, A.; Angelini, D.; Glaros, T.; Cole, S. *Role of Acetylcholinesterase in the Regulation of Human Mesenchymal Stem Cell Proliferation and Differentiation*; ECBC-TR-1346; U.S. Army Edgewood Chemical Biological Center: Aberdeen Proving Ground, MD, 2016; UNCLASSIFIED Report.

30. Angelini, D.J.; Su, Q.; Kolosova, I.A.; Fan, C.; Skinner, J.T.; Yamaji-Kegan, K.; Collector, M.; Sharkis, S.J.; Johns, R.A. Hypoxia-Induced Mitogenic Factor (HIMF/FIZZ1/RELM alpha) Recruits Bone Marrow-Derived Cells to the Murine Pulmonary Vasculature. *PLoS One* **2010,** *5*, e11251.

31. Kolosova, I.A.; Angelini, D.; Fan, C.; Skinner, J.; Cheadle, C.; Johns, R.A. Resistin-Like Molecule Alpha Stimulates Proliferation of Mesenchymal Stem Cells while Maintaining Their Multipotency. *Stem Cells Dev.* **2013,** *22*, 239–247.

32. Ke, N.; Wang, X.; Xu, X.; Abassi, Y.A. The xCELLigence System for Real-Time and Label-Free Monitoring of Cell Viability. *Methods Mol. Biol.* **2011,** *740,* 33–43.

33. Wisniewski, J.R.; Zougman, A.; Nagaraj, N.; Mann, M. Universal Sample Preparation Method for Proteome Analysis. *Nat. Methods* **2009,** *6*, 359–362.

34. Keshishian, H.; Burgess, M.W.; Gillette, M.A.; Mertins, P.; Clauser, K.R.; Mani, D.R.; Kuhn, E.W.; Farrell, L.A.; Gerszten, R.E.; Carr, S.A. Multiplexed, Quantitative Workflow for Sensitive Biomarker Discovery in Plasma Yields Novel Candidates for Early Myocardial Injury. *Mol. Cell Proteomics* **2015,** *14*, 2375–2393.

35. Wang, Y.; Yang, F.; Gritsenko, M.A.; Wang, Y.; Clauss, T.; Liu, T.; Shen, Y.; Monroe, M.E.; Lopez-Ferrer, D.; Reno, T.; Moore, R.J.; Klemke, R.L.; Camp, D.G. II; Smith, R.D. Reversed-Phase Chromatography with Multiple Fraction Concatenation Strategy for Proteome Profiling of Human MCF10A Cells. *Proteomics* **2011,** *11*, 2019–2026.

36. Mayeux-Portas, V.; File, S.E.; Stewart, C.L.; Morris, R.J. Mice Lacking the Cell Adhesion Molecule Thy-1 Fail to Use Socially Transmitted Cues to Direct Their Choice of Food. *Curr. Biol.* **2000,** *10*, 68–75.

37. Rege, T.A.; Hagood, J.S. Thy-1, A Versatile Modulator of Signaling Affecting Cellular Adhesion, Proliferation, Survival, and Cytokine/Growth Factor Responses. *Biochim. Biophys. Acta* **2006,** *1763*, 991–999.

38. Rege, T.A.; Hagood, J.S. Thy-1 as a Regulator of Cell-Cell and Cell-Matrix Interactions in Axon Regeneration, Apoptosis, Adhesion, Migration, Cancer, and Fibrosis. *FASEB J.* **2006,** *20*, 1045–1054.

39. Rege, T.A.; Pallero, M.A.; Gomez, C.; Grenett, H.E.; Murphy-Ullrich, J.E.; Hagood, J.S. Thy-1, via Its GPI Anchor, Modulates Src Family Kinase and Focal Adhesion Kinase Phosphorylation and Subcellular Localization, and Fibroblast Migration, in Response to Thrombospondin-1/hep I. *Exp. Cell. Res.* **2006,** *312,* 3752–3767.

40. Cooke, G.; Armstrong, M.E.; Donnelly, S.C. Macrophage Migration Inhibitory Factor (MIF), Enzymatic Activity and the Inflammatory Response. *Biofactors* **2009,** 35, 165–168.

41. Larson, D.F.; Horak, K. Macrophage Migration Inhibitory Factor: Controller of Systemic Inflammation. *Crit. Care* **2006,** *10*, 138.

42. Saba-El-Leil, M.K.; Fremin, C.; Meloche, S. Redundancy in the World of MAP Kinases: All for One. *Front. Cell. Dev. Biol.* **2016,** *4*, 67.

43. Huang, B.; Porter, G. Expression of Proline-Rich Akt-Substrate PRAS40 in Cell Survival Pathway and Carcinogenesis. *Acta Pharmacol. Sin.* **2005,** *26*, 1253–1258.

44. Frame, S.; Cohen, P. GSK3 Takes Centre Stage More than 20 Years after Its Discovery. *Biochem. J.* **2001,** *359*, 1–16.

45. Mounier, N.; Arrigo, A.P. Actin Cytoskeleton and Small Heat Shock Proteins: How Do They Interact? *Cell. Stress Chaperones* **2002,** *7*, 167–176.

46. Tu, S.W.; Bugde, A.; Luby-Phelps, K.; Cobb, M.H. WNK1 Is Required for Mitosis and Abscission. *Proc. Natl. Acad. Sci. USA* **2011,** *108*, 1385–1390.

47. Mori, T.; Li, Y.; Hata, H.; Kochi, H. NIRF Is a Ubiquitin Ligase that is Capable of Ubiquitinating PCNP, a PEST-Containing Nuclear Protein. *FEBS Lett.* **2004,** *557*, 209–214.

48. Coppola, T.; Magnin-Luthi, S.; Perret-Menoud, V.; Gattesco, S.; Schiavo, G.; Regazzi, R. Direct Interaction of the Rab3 Effector RIM with Ca2+ Channels, SNAP-25, and Synaptotagmin. *J. Biol. Chem.* **2001,** *276*, 32756–32762.

49. Lattanzio, R.; Piantelli, M.; Falasca, M. Role of Phospholipase C in Cell Invasion and Metastasis. *Adv. Biol. Regul.* **2013,** *53*, 309–318.

50. Uliczka, F.; Kornprobst, T.; Eitel, J.; Schneider, D.; Dersch, P. Cell Invasion of Yersinia pseudotuberculosis by Invasin and YadA Requires Protein Kinase C, Phospholipase C-gamma1 and Akt Kinase. *Cell. Microbiol.* **2009,** *11*, 1782–1801.

51. Takegahara, N.; Kang, S.; Nojima, S.; Takamatsu, H.; Okuno, T.; Kikutani, H.; Toyofuku, T.; Kumanogoh, A. Integral Roles of a Guanine Nucleotide Exchange Factor, FARP2, in Osteoclast Podosome Rearrangements. *FASEB J.* **2010,** *24*, 4782–4792.

52. Stanton, S.E.; McReynolds, L.J.; Evans, T.; Schreiber-Agus, N. Yaf2 Inhibits Caspase 8-Mediated Apoptosis and Regulates Cell Survival during Zebrafish Embryogenesis. *J. Biol. Chem.* **2006,** *281*, 28782–28793.

53. Jeronimo, C.; Langelier, M.F.; Zeghouf, M.; Cojocaru, M.; Bergeron, D.; Baali, D.; Forget, D.; Mnaimneh, S.; Davierwala, A.P.; Pootoolal, J.; Chandy, M.; Canadien, V.; Beattie, B.K.; Richards, D.P.; Workman, J.L.; Hughes, T.R.; Greenblatt, J.; Coulombe, B. RPAP1, a Novel Human RNA Polymerase II-Associated Protein Affinity Purified with Recombinant Wild-Type and Mutated Polymerase Subunits. *Mol. Cell. Biol.* **2004,** *24*, 7043–7058.

54. Xie, X.; Wang, Z.; Chen, Y. Association of LKB1 with a WD-Repeat Protein WDR6 Is Implicated in Cell Growth Arrest and p27(Kip1) Induction. *Mol. Cell. Biochem*. **2007,** *301*, 115–122.

55. Minocherhomji, S.; Hansen, C.; Kim, H.G.; Mang, Y.; Bak, M.; Guldberg, P.; Papadopoulos, N.; Eiberg, H.; Doh, G.D.; Mollgard, K.; Hertz, J.M.; Nielson, J.E.; Ropers, H.H.; Turner, Z.; Tommerup, N.; Kalscheuer, V.M.; Silahtaroglu, A. Epigenetic Remodelling and Dysregulation of DLGAP4 Is Linked with Early-Onset Cerebellar Ataxia. *Hum. Mol. Genet.* **2014,** *23*, 6163–6176.

56. Brooks, S.A.; Blackshear, P.J. Tristetraprolin (TTP): Interactions with mRNA and Proteins, and Current Thoughts on Mechanisms of Action. *Biochim. Biophys. Acta* **2013,** *1829*, 666–679.

57. Young, D.J.; Stoddart, A.; Nakitandwe, J.; Chen, S.C.; Qian, Z.; Downing, J.R.; Le Beau, M.M. Knockdown of Hnrnpa0, a del(5q) Gene, Alters Myeloid Cell Fate in Murine Cells through Regulation of AU-Rich Transcripts. *Haematologica* **2014,** *99*, 1032–1040.

58. Sharma, P.; Bolten, Z.T.; Wagner, D.R.; Hsieh, A.H. Deformability of Human Mesenchymal Stem Cells Is Dependent on Vimentin Intermediate Filaments. *Ann. Biomed. Eng.* **2017**.

59. Vilchez, D.; Boyer, L.; Morantte, I.; Lutz, M.; Merkwirth, C.; Joyce, D.; Spencer, B.; Page, L.; Masliah, E.; Berggren, W.T.; Gage, F.H.; Dillin, A. Increased Proteasome Activity In Human Embryonic Stem Cells Is Regulated by PSMD11. *Nature* **2012,** *489*, 304–308.

60. Pallen, M.J. Glucoamylase-Like Domains in the Alpha- and Beta-Subunits of Phosphorylase Kinase. *Protein Sci*. **2003,** *12*, 1804–1807.

61. Yang, K.; Shen, J.; Chen, S.W.; Qin, J.; Zheng, X.Y.; Xie, L.P. Upregulation of PAWR by Small Activating RNAs Induces Cell Apoptosis in Human Prostate Cancer Cells. *Oncol. Rep.* **2016,** *35*, 2487–2493.

62. Peng, X.; Nelson, E.S.; Maiers, J.L.; DeMali; K.A. New Insights into Vinculin Function and Regulation. *Int. Rev. Cell. Mol. Biol.* **2011,** *287*, 191–231.

63. Kezic, S.; Jakasa, I. Filaggrin and Skin Barrier Function. *Curr. Probl. Dermatol*. **2016,** *49*, 1–7.

64. Kuechle, M.K.; Presland, R.B.; Lewis, S.P.; Fleckman, P.; Dale, B.A. Inducible Expression of Filaggrin Increases Keratinocyte Susceptibility to Apoptotic Cell Death. *Cell Death Differ*. **2000,** *7*, 566–573.

65. Vinik, Y.; Shatz-Azoulay, H.; Vivanti, A.; Hever, N.; Levy, Y.; Karmona, R.; Brumfeld, V.; Baraghithy, S.; Attar-Lamdar, M.; Boura-Halfon, S.; Bab, L.; Zick, Y. The Mammalian Lectin Galectin-8 Induces RANKL Expression, Osteoclastogenesis, and Bone Mass Reduction in Mice. *Elife* **2015,** *4*, e05914.

66. Sun, Y.; Sukumaran, P.; Schaar, A.; Singh, B.B. TRPM7 and Its Role in Neurodegenerative Diseases. *Channels (Austin)* **2015,** *9*, 253–261.

67. Visser, D.; Middelbeek, J.; van Leeuwen, F.N.; Jalink, K. Function and Regulation of the Channel-Kinase TRPM7 in Health and Disease. *Eur. J. Cell. Biol.* **2014,** 93, 455–465.

68. Di Martino, J.; Paysan, L.; Gest, C.; Lagree, V.; Juin, A.; Saltel, F.; Moreau, V. Cdc42 and Tks5: A Minimal and Universal Molecular Signature for Functional Invadosomes. *Cell. Adh. Migr.* **2014,** *8*, 280–292.

69. Dikic, I. CIN85/CMS Family of Adaptor Molecules. *FEBS Lett.* **2002,** *529*, 110–115.

70. Arif, A.; Jia, J.; Mukhopadhyay, R.; Willard, B.; Kinter, M.; Fox, P.L. Two-Site Phosphorylation of EPRS Coordinates Multimodal Regulation of Noncanonical Translational Control Activity. *Mol. Cell.* **2009,** *35*, 164–180.

71. Markert, A.; Grimm, M.; Martinez, J.; Wiesner, J.; Meyerhans, A.; Meyuhas, O.; Sickmann, A.; Fischer, U. The La-Related Protein LARP7 is a Component of the 7SK Ribonucleoprotein and Affects Transcription of Cellular and Viral Polymerase II Genes. *EMBO Rep.* **2008,** *9*, 569–575.

72. Mukudai, Y.; Kondo, S.; Fujita, A.; Yoshihama, Y.; Shirota, T.; Shintani, S. Tumor Protein D54 Is a Negative Regulator of Extracellular Matrix-Dependent Migration and Attachment in Oral Squamous Cell Carcinoma-Derived Cell Lines. *Cell. Oncol. (Dordr)* **2013,** *36*, 233–245.

73. Ayala, Y.R.; Conn, P.M. Protein Disulfide Isomerase Chaperone ERP-57 Decreases Plasma Membrane Expression of the Human GnRH Receptor. *Cell. Biochem. Funct.* **2010,** *28*, 66–73.

74. Zhuang, B.; Su, Y.S.; Sockanathan, S. FARP1 Promotes the Dendritic Growth of Spinal Motor Neuron Subtypes through Transmembrane Semaphorin6A and PlexinA4 Signaling. *Neuron* **2009,** *61*, 359–372.

ACRONYMS AND ABBREVIATIONS

Ach	acetylcholine
AChE	acetylcholinesterase
ATP	adenosine triphosphate
bRPLC	basic reverse-phase liquid chromatography
CANX	calnexin
CD	cluster of differentiation
CI	cell index
CWA	chemical warfare agent
DLGAP4	disks large-associated protein 4
ECBC	U.S. Army Edgewood Chemical Biological Center
EIF4G1	eukaryotic initiation factor 4G
EPRS	bifunctional glutamate/proline—tRNA ligase
ERK1/2	extracellular signal-regulated kinases 1/2
FARP1	FERM, RhoGEF and pleckstrin domain-containing protein 1
FARP2	FERM, RhoGEF and pleckstrin domain-containing protein 2
FLG	filaggrin
GSK3α/β	glycogen synthase 3 alpha/beta
GTP	guanosine 5'-triphosphate
hnRNP A0	heterogeneous nuclear ribonucleoprotein A0
HSP27	heat shock protein 27
LARP7	La-related protein 7
LC–MS	liquid chromatography–mass spectrometry
OP	organophosphorus
MIF	macrophage migration inhibitory factor
MSC	mesenchymal stem cell
MRC2	C-type mannose receptor 2
MS2	tandem mass spectrometry
m/z	mass-to-charge ratio
PAWR	PRKC apoptosis WT1 regulator protein
PCNP	1-phosphatidylinositol-4,5-bisphosphate phosphodiesterase gamma-1 isoform α
PHKB	phsophorylase b kinase regulatory subunit β
PRAS40	proline-rich Akt substrate 40
PSMD11	26S proteasome non-ATPase regulatory subunit 11
RIMS1	regulating synaptic membrane exocytosis protein 1 isoform 2
RNA	ribonucleic acid
RPAP1	RNA polymerase II-associated protein 1
RTCA	real time cell analyzer
SH3KBP1	src homology 3 domain-containing kinase-binding protein 1
SH3PXD2A	src homology 3 and phox homology domain-containing protein 2A
TEAB	triethylammonium bicarbonate
TPD52L2	tumor protein D54
TRPM7	transient receptor potential cation channel subfamily M member 7

TMT	tandem mass tag
WDR6	WD repeat-containing protein 6
WNK1	WNK lysine deficient protein kinase 1
VCL	vinculin
VIM	vimentin
VX	*O*-ethyl-*S*-[2(diisopropylamino)ethyl]methyl-phosphononthioate
YAF2	YY1-associated factor 2 isoform 1
ZFP36	mRNA decay activator protein ZFP36

DISTRIBUTION LIST

The following individuals and organizations were provided with one Adobe portable document format (pdf) electronic version of this report:

U.S. Army Edgewood Chemical
Biological Center (ECBC)
RDCB-DRB-D
ATTN: Angelini, D.
Glaros, T.
Prugh, A.
Rosenzweig, N.
Basi, Kelly
RDCB-DRT-M
ATTN: Phillips, C.
Kristovich, R.

Department of Homeland Security
RDCB-PI-CSAC
ATTN: Negron, A.
DHS-S&T-RDP-CSAC
ATTN: Strang, P.

G-3 History Office
U.S. Army RDECOM
ATTN: Smart, J.

ECBC Technical Library
RDCB-DRB-BL
ATTN: Foppiano, S.
Stein, J.

Office of the Chief Counsel
AMSRD-CC
ATTN: Upchurch, V.

Defense Technical Information Center
ATTN: DTIC OA

ECBC Rock Island
RDCB-DES
ATTN: Lee, K.
RDCB-DEM
ATTN: Grodecki, J.


EDGEWOOD CHEMICAL BIOLOGICAL CENTER
A U.S. Army RDECOM Laboratory